Supplementary Materials

Supplement 1 Range of dates for mapping western Hudson Bay flaw lead

This supplement includes a range of dates with >95% of the Hudson Bay coastline bordered by landfast ice used to map the flaw lead (Table S1).

Table S1. Range of dates with > 95% of the Hudson Bay coastline bordered by landfast ice used to map the flaw lead. Landfast ice was extracted from biweekly (January–March, 2010–2011) and weekly (March–December, 2010-2011; January-December 2012-2018) Canadian Ice Service Hudson Bay Arctic Regional Sea Ice Charts in SIGRID-3 Format (Canadian Ice Service 2009).

Year	Start	End
2010	2009-12-21	2010-04-26
2011	2011-01-17	2011-05-16
2012	2011-12-26	2012-05-07
2013	2012-12-31	2013-05-13
2014	2013-12-16	2014-05-19
2015	2014-12-15	2015-05-04
2016	2015-12-28	2016-05-16
2017	2016-12-26	2017-05-22
2018	2017-12-25	2018-05-21

Supplement 2 Western Hudson Bay Flaw Lead Width

This supplement contains an example of how the width of the western Hudson Bay flaw lead was calculated (Fig. S1), and tables from the Wilcoxon signed rank test comparing the maximum width and total area of the western Hudson Bay flaw lead by month (Tables S2 and S3; Fig. S2).

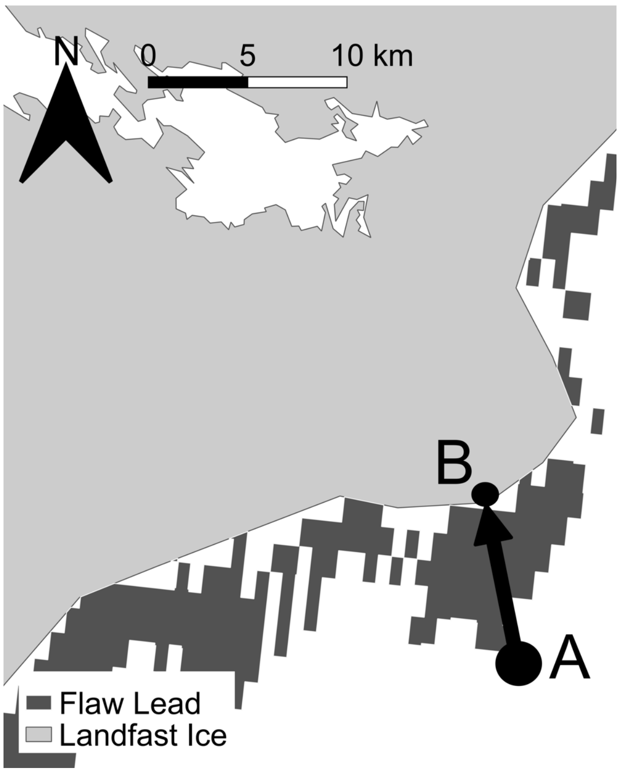

Fig. S1. Example of calculating the width of the western Hudson Bay flaw lead. The maximum width was calculated as the straight-line distance from the edge of the flaw lead (A) to the closest point on the landfast ice (B). The flaw lead was mapped using synthetic aperture radar imagery from December–May, 2009–2018. Landfast ice was extracted from the Canadian Ice Service Hudson Bay Arctic Regional Sea Ice Charts in SIGRID-3 Format (Canadian Ice Service 2009). Weekly sea ice charts were available for the whole period except January–March of 2010–2011, when biweekly sea ice charts were used. The width closest to the Western Hudson Bay adult female polar bears' position was calculated in the same manner. Adult female polar bears are from the Western Hudson Bay subpopulation, from December–May, 2009–2018.

Table S2. Comparison of the maximum width of the western Hudson Bay flaw lead by month. Data were based on synthetic aperture radar images from December–May, 2011, 2013–2018. 2010 and 2012 were excluded from analysis as there were no images for May 2010 or April 2012. Width was compared using a Wilcoxon signed-rank test (α = 0.05). There was no significant difference in the maximum width in December and January (Wilcoxon signed-rank $z = -0.05$, $p = 0.96$), therefore months values were combined due December being represented by only 23 images from the last two weeks. Presented values are the median maximum width (km).

	Median Maximum Width (km)	February		March		April		May	
		p value	r	*p* value	r	*p* value	r	*p* value	r
Dec/Jan	20	0.07	0.17	0.03	0.20	0.20	0.12	<0.001	0.56
Feb	15	-		0.94	0.01	<0.001	0.38	<0.001	0.59
Mar	16			-		<0.001	0.33	<0.001	0.57
Apr	24					-		<0.001	0.54
May	53							-	

Table S3. Comparison of the total area of the western Hudson Bay flaw lead. Data were based on synthetic aperture radar images from December to May, 2011, 2013–2018. 2010 and 2012 were excluded from analysis as there were no images for May 2010 or April 2012. Area was compared using a Wilcoxon signed-rank test (α = 0.05). There was no significant difference in the total area in December and January (Wilcoxon signed-rank $z = -0.88$, $p = 0.37$), therefore these months were combined due December being represented by only 23 images from the last two weeks. Presented values are the median total area (km^2).

	Median Total Area (km^2)	February		March		April		May	
		p value	r	*p* value	r	*p* value	r	*p* value	r
Dec/Jan	2821	0.03	0.20	<0.001	0.38	0.67	0.04	<0.001	0.38
Feb	1484	-		0.09	0.16	<0.001	0.33	<0.001	0.54
Mar	1471			-		<0.001	0.43	<0.001	0.55
Apr	2902					-		<0.001	0.42
May	6469							-	

A

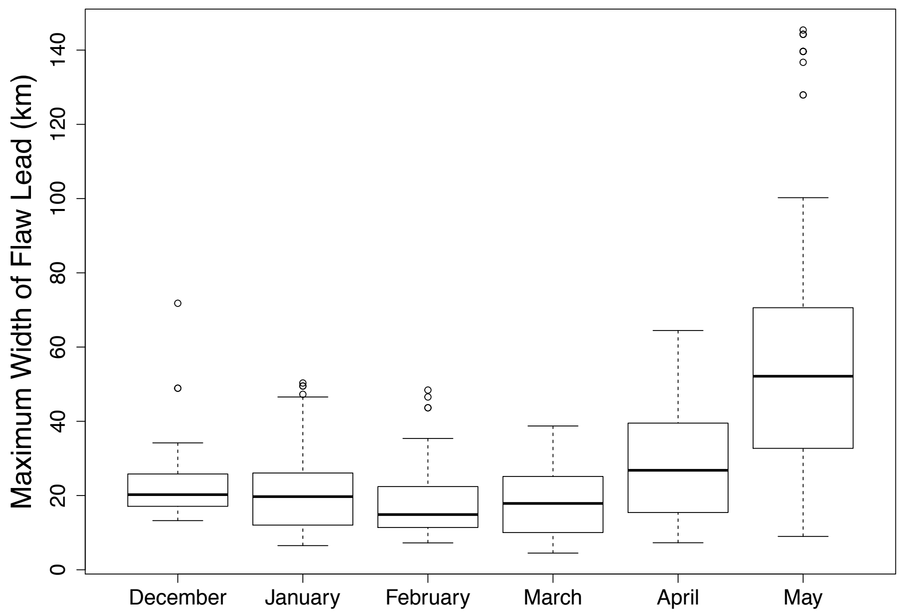

B

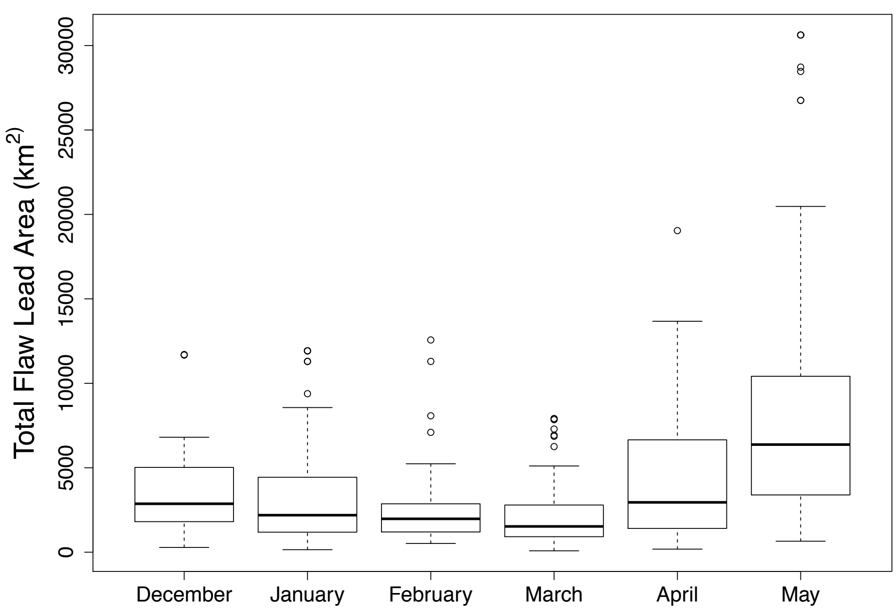

Fig. S2. Comparison of the western Hudson Bay flaw lead A) maximum width (km) and B) total area (km^2) by month from December–May, 2009–2018. The flaw lead was mapped using synthetic aperture radar. December and January were compared using a Wilcoxon signed-rank test ($\alpha = 0.05$) and determined to not significantly differ in maximum width (Wilcoxon signed-rank z = -0.05, p = 0.96), or total area (Wilcoxon signed-rank z =-0.88, p = 0.37), therefore these months were combined due December being represented by only 23 images from the last two weeks.

Supplement 3 Selection of the western Hudson Bay flaw lead

This supplement contains Akaike Information Criterion results for selection of the top generalized linear mixed effects models with a binomial link predicting the selection of the western Hudson Bay flaw lead by Western Hudson Bay polar bears based on flaw lead width closest to the bear in a used and available design. Candidate Models and Akaike Information Criterion results are presented in Table S4.

Table S4. Akaike Information Criterion results for the top candidate models predicting the selection of the western Hudson Bay flaw lead by Western Hudson Bay polar bears based on flaw lead width closest to the bear in a used and available design using a general linear mixed effects model. Adult female polar bears are from the Western Hudson Bay subpopulation, from January 2010–May 2018. Individual bear identification was the random effect. K is the number of random effects terms, AIC_c is the corrected Akaike Information Criterion score for each model, ΔAIC_c is the difference in AIC_c scores between the top model and subsequent candidate models, w is the AIC weight, and LL is the log likelihood value. Width is the width of the flaw lead at the point closest to the bear and random locations. The flaw lead was mapped using synthetic aperture radar.

Rank	Model	k	AIC_c	ΔAIC_c	w	LL
Selection of Flaw Lead ($n_{locations}$ = 8083)						
1	Width	2	2346	0.0	1	-1170

Supplement 4 χ^2 tests without locations on landfast ice

This supplement contains the results of χ^2 tests without locations on landfast ice (Table S5).

Table S5. Standardized residuals of χ^2 analyses comparing the proportion of adult female polar bear locations on, near, and off the western Hudson Bay flaw lead of all bears, by reproductive status, and by month without locations on landfast ice. Positive bolded values are where bears are spending more time than expected, negative bolded values bears are spending less time than expected based on the habitat available. Solitary = solitary adult females, COY = females with cub(s)-of-the-year, and YRLG = females with yearling(s).

	On	Near	Off	χ^2	df	*p* value
Solitary	**2.7**	**18.8**	**-18.0**	366	2	<0.001
COY	-1.0	**-5.2**	**5.2**	29	2	<0.001
YRLG	-0.5	**4.7**	**-3.9**	22	2	<0.001
All	**2.2**	**9.3**	**-9.4**	93	2	<0.001

	December	January	February	March	April	May	χ^2	df	*p* value
On	**-8.0**	**-2.0**	**-5.8**	**2.3**	**7.5**	**5.0**	156	5	<0.001
Near	**-16.0**	**-14.7**	**-11.0**	3.5	**10.3**	**27.3**	1207	5	<0.001
Off	**5.5**	**4.3**	**3.7**	**-1.2**	**-3.8**	**-8.5**	8698	5	<0.001

Supplement 5 Habitat quality and floe size

This supplement contains candidate models and results of Akaike Information Criterion used to select the top generalized linear mixed effects models predicting habitat quality and floe size based on distance to the western Hudson Bay flaw lead (Table S6).

Table S6. Candidate models and Akaike Information Criterion values for models predicting habitat quality and floe size adult female polar bears used with a generalized linear mixed effects model. Adult female polar bears are from the Western Hudson Bay subpopulation, from December to May, 2009–2018. Individual bear identification was the random effect. k is the number of random effects terms, AIC_c is the corrected Akaike Information Criterion score for each model, ΔAIC_c is the difference in AIC_c scores between the top model and subsequent candidate models, w is the AIC_c weight, and LL is the log likelihood value. dist_ld is the bear distance to the flaw lead. Habitat was classified as nonoptimal (ice concentration ≤60%) or optimal (ice concentration >60%) based on Canadian Ice Service Hudson Bay Arctic Regional Sea Ice Charts in SIGRID-3 Format (Canadian Ice Service 2009). Floe size was classified as medium or big (floes characterized as big or vast were included in the big category; Canadian Ice Service 2009) . The flaw lead was mapped using synthetic aperture radar.

Rank	Model	k	AIC_c	ΔAIC_c	w	LL
Habitat Quality ($n_{locations}$ = 13 516)						
1	dist_ld	3	590.8	0.0	0.51	-292
2	dist_ld + $dist\_ld^2$	4	590.0	0.1	0.49	-291
Floe Size ($n_{locations}$ = 13 436)						
1	dist_ld	3	1894	0.0	0.95	- 944
2	dist_ld + $dist\_ld^2$	4	1900	5.7	1.00	- 946

Supplement 6 Distance to the western Hudson Bay flaw lead and landfast ice

This supplement includes methods predicting adult female western Hudson Bay polar bears' distance to western Hudson Bay landfast ice (hereafter landfast ice), as well as tables of all candidate models predicting distance to the western Hudson Bay flaw lead and landfast ice (Table S7), Akaike Information Criterion results (flaw lead: Table S8; landfast ice: Table S10), the results of all models predicting distance to the flaw lead run with and without locations on landfast ice (Tables S8 and S9), and results predicting bears' distance to landfast ice (Table S11). This supplement also contains a figure (Fig. S3) showing bears' distance to the flaw lead. Adult female polar bears are from the Western Hudson Bay subpopulation, from December to May, 2009–2018 and the flaw lead was mapped using synthetic aperture radar.

We used maximum likelihood, linear mixed effects (LME) models to predict bears' distance landfast ice based on maximum daily FL width, total daily FL area, month, and reproductive status with a random effect for bear (Table 1). Distance to landfast ice was calculated as the shortest straight-line distance from the bear location to the closest point on the landfast ice. Distinct months provided a better fit than linear or quadratic transformed ordinal date or ordered date (beginning first day landfast ice bordered >95% of Hudson Bay coastline in December to the last day in April/May for each year), so it was used in candidate models. Maximum daily FL width and total daily FL area were included as linear and quadratic variables. As females with COY return to ice in March (Stirling et al. 1977, Ramsay & Andriashek 1986), bringing them closer in proximity to the FL, we determined whether month and reproductive status influenced distance to the FL both individually and as an interaction. We excluded females with YRLG from December to February because there was only one in these months. Models were fit predicting both distance to landfast ice to assess whether the bears moved closer to the FL, or the FL edge became closer to bears as it widened.

Predictor variables were tested for correlation using a Spearman's rank correlation coefficient, to exclude correlated variables ($r > |0.6|$) from the same models. Corrected Akaike Information Criterion values (AIC_c) were used for model selection; if ΔAIC_c was <2, the most parsimonious model was selected as the top model (Burnham & Anderson 2002). Significance of top model predictor variables were assessed at $\alpha = 0.05$. Models were repeated without locations on landfast ice to test whether bears' use was affected by the FL when on landfast ice.

Similar results were observed when predicting bears' distance to landfast ice as when predicting bears distance to the flaw lead, except bears were closer to the FL on days with a narrower FL (Table S9 in Supplement 6). This suggests bears were moving closer to the flaw lead, rather than the flaw lead edge moved closer to the bears as the feature widened.

Table S7. Candidate models predicting adult female polar bear distance to the western Hudson Bay flaw lead and landfast ice using a linear mixed effects model. Individual bear identification was the random effect. Month represents 6 categories (December–May inclusive). RS represents reproductive status with 3 categories; females with cub(s)-of-the-year (Dec: $n_{bears} = 21$; Jan: $n_{bears} = 23$; Feb: $n_{bears} = 20$; Mar: $n_{bears} = 20$; Apr: $n_{bears} = 17$; May: $n_{bears} = 16$), females with yearling(s; Mar: $n_{bears} = 24$; Apr: $n_{bears} = 26$; May: $n_{bears} = 23$), and solitary females (Dec: $n_{bears} = 2$; Jan: $n_{bears} = 4$; Feb: $n_{bears} = 5$; Mar: $n_{bears} = 39$; Apr: $n_{bears} = 39$; May: $n_{bears} = 31$). There was one female with yearling(s) from December–February, therefore these locations were removed from analysis. ar_dl is the total area and wd_dl is the maximum width of the flaw lead.

Model	Predictor Variables
December–May	
1	Month
2	wd_dl
3	wd_dl + wd_dl^2
4	ar_dl
5	ar_dl + ar_dl^2
6	RS
7	Month + RS
8	wd_dl + RS
9	wd_dl + wd_dl^2 + RS
10	ar_dl + RS
11	ar_dl + ar^2 + RS
12	Month + RS + Month*RS
13	Month + wd_dl
14	Month + wd_dl + wd_dl^2
15	Month + ar_dl
16	Month + ar_dl + ar_dl^2
17	Month + RS + wd_dl
18	Month + RS + wd_dl + wd_dl^2
19	Month + RS + ar_dl
20	Month + RS+ ar_dl + ar_dl^2
21	Month + RS + Month*RS + wd_dl
22	Month + RS + Month*RS + wd_dl + wd_dl^2
23	Month + RS + Month*RS + ar_dl
24	Month + RS + Month*RS + ar_dl + ar_dl^2

Table S8. Akaike Information Criterion results for the top 5 candidate models predicting adult female polar bear distance to the flaw lead with and without locations on western Hudson Bay landfast ice using a linear mixed effects model. Individual bear identification was the random effect. k is the number of random effects terms, AIC_c is the corrected Akaike Information Criterion score for each model, ΔAIC_c is the difference in AIC_c scores between the top model and subsequent candidate models, w is the AIC_c weight, and LL is the log likelihood value. Month represents 6 categories (December–May inclusive). RS represents reproductive status with 3 categories; females with cub(s)-of-the-year (Dec: n_{bears} = 21; Jan: n_{bears} = 23; Feb: n_{bears} = 20; Mar: n_{bears} = 20; Apr: n_{bears} = 17; May: n_{bears} = 16), females with yearling (s; Mar: n_{bears} = 24; Apr: n_{bears} = 26; May: n_{bears} = 23), and solitary females (Dec: n_{bears} = 2; Jan: n_{bears} = 4; Feb: n_{bears} = 5; Mar: n_{bears} = 39; Apr: n_{bears} = 39; May: n_{bears} = 31). There was only one female with yearling(s) from December–February, therefore these locations were removed from analysis. Ar_dl is the total area and wd_dl is the maximum width of the flaw lead.

Rank	Model	k	AIC_c	ΔAIC_c	w	LL
December–May ($n_{locations}$ = 16 058)						
1	Month + RS + Month*RS + wd_dl + wd_dl^2	19	180768	0.0	1.0	-90365
2	Month + RS + Month*RS + ar_dl + ar_dl^2	19	180785	16	0.0	-90373
3	Month + RS + Month*RS + wd_dl	18	180808	40	0.0	-90386
4	Month + RS + Month*RS + ar_dl	18	180817	48	0.0	-90390
5	Month + RS + Month*RS	17	180912	144	0.0	-90439
December–May Without Locations on Landfast Ice ($n_{locations}$ = 15 864)						
1	Month + RS + Month*RS + wd_dl + wd_dl^2	19	178435	0.0	0.9	-89197
2	Month + RS + Month*RS + ar_dl + ar_dl^2	19	178439	3	0.1	-89200
3	Month + RS + Month*RS + wd_dl	18	178466	31	0.0	-89215
4	Month + RS + Month*RS + ar_dl	18	178468	32	0.0	- 89216
5	Month + RS + Month*RS	17	178572	137	0.0	- 89269

Table S9. Covariate coefficient estimates for the top models predicting adult female polar bear distance to the flaw lead with and without locations on western Hudson Bay landfast ice using a maximum likelihood linear mixed effects model (α = 0.05). YRLG represents females with yearling(s), and COY represents females with cub(s)-of-the-year. Max width is the maximum width of the flaw lead. There was only one female with yearling(s) from December–February, therefore these locations were removed from analysis.

				95% CI		
Model	Parameter	Estimate	SE	Lower	Upper	*p* value
Distance to FL With All Locations	December	136.6	4.7	127.4	145.9	<0.001
	January	57.5	3.7	50.2	64.8	<0.001
	February	17.6	3.8	10.1	25.2	<0.001
	March	-11.5	3.8	-18.9	-4.0	<0.01
	April	16.8	3.4	10.2	23.4	<0.001
	COY & May	161.2	11.2	139.3	183.1	<0.001
	Solitary	-3.5	3.4	-10.0	3.1	>0.05
	YRLG	-11.3	3.7	-18.5	-4.1	<0.01
	Daily Width	-4.9E-04	4.3E-05	-5.8E-04	-4.1E-04	<0.001
	Daily Width^2	5.1E-04	7.8E-05	4.8E-05	8.9E-05	<0.001
	Dec*Solitary	-93.1	15.2	-123.0	-63.2	<0.001
	Jan*Solitary	-10.7	6.4	-23.3	1.8	>0.05
	Feb*Solitary	46.6	6.1	34.7	58.5	<0.001
	Mar*Solitary	52.0	4.3	43.5	60.4	<0.001
	Apr*Solitary	21.4	4.0	13.6	29.2	<0.001
	Mar*YRLG	30.1	4.6	21.1	39.1	<0.001
	Apr*YRLG	11.8	4.3	3.4	20.3	<0.01
Distance to FL Without Locations on Landfast Ice	December	136.5	4.7	127.3	145.7	<0.001
	January	57.5	3.7	50.2	64.8	<0.001
	February	17.8	3.8	10.4	25.3	<0.001
	March	-9.0	3.8	-16.5	-1.5	<0.05
	April	17.6	3.4	11.0	24.2	<0.001
	COY & May	161.3	11.2	139.4	183.2	<0.001
	Solitary	-0.8	3.4	-7.3	5.8	>0.05
	YRLG	-10.4	3.7	-17.5	-3.2	<0.01
	Daily Width	-4.7E-04	4.3E-05	-5.5E-04	-3.8E-04	<0.001
	Daily Width^2	6.0E-05	1.1E-05	4.0E-05	8.1E-05	<0.001
	Dec*Solitary	-100.1	15.2	-129.9	-70.3	<0.001
	Jan*Solitary	-17.3	6.4	-29.8	-4.7	<0.01
	Feb*Solitary	40.8	6.1	28.9	52.8	<0.001
	Mar*Solitary	46.8	4.3	38.3	55.3	<0.001
	Apr*Solitary	18.2	4.0	10.4	26.1	<0.001
	Mar*YRLG	26.4	4.6	17.3	35.4	<0.001
	Apr*YRLG	12.3	4.3	3.9	20.8	<0.01

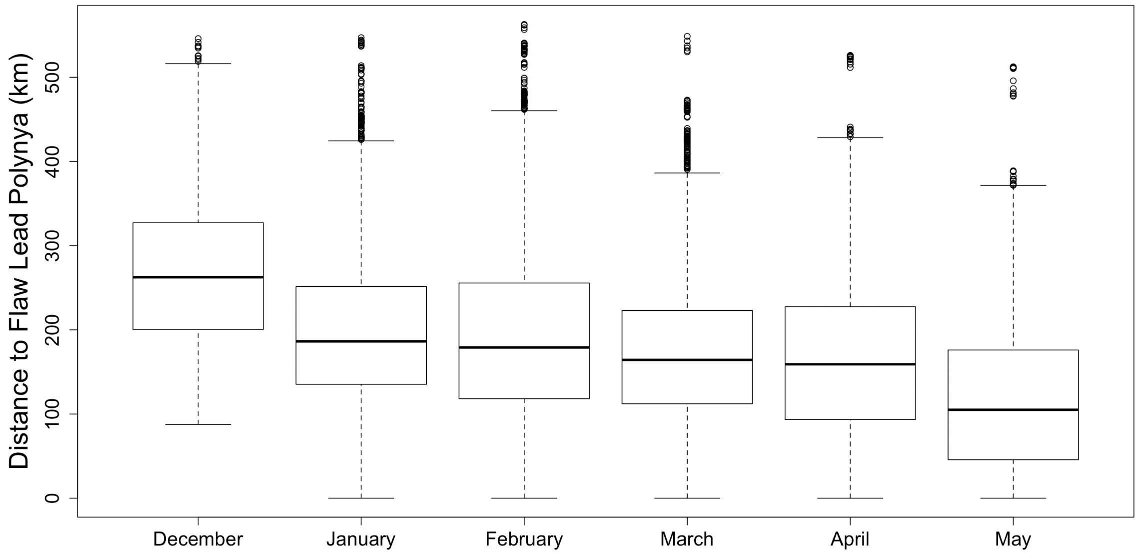

Fig. S3. Western Hudson Bay adult female polar bears' distance (km) to the western Hudson Bay flaw lead by month from December–May, 2009–2018.

Table S10. Akaike Information Criterion results for the top 5 candidate models predicting adult female polar bear distance to western Hudson Bay landfast ice with and without locations on Western Hudson Bay landfast ice using a linear mixed effects model. Individual bear identification was the random effect. k is the number of random effects terms, AIC_c is the corrected Akaike Information Criterion score for each model, ΔAIC_c is the difference in AIC_c scores between the top model and subsequent candidate models, w is the AIC_c weight, and LL is the log likelihood value. Month represents 6 categories (December–May inclusive). RS represents reproductive status with 3 categories; females with cub(s)-of-the-year (Dec: n_{bears} = 21; Jan: n_{bears} = 23; Feb: n_{bears} = 20; Mar: n_{bears} = 20; Apr: n_{bears} = 17; May: n_{bears} = 16), females with yearling(s; Mar: n_{bears} = 24; Apr: n_{bears} = 26; May: n_{bears} = 23), and solitary females (Dec: n_{bears} = 2; Jan: n_{bears} = 4; Feb: n_{bears} = 5; Mar: n_{bears} = 39; Apr: n_{bears} = 39; May: n_{bears} = 31). There was only one female with yearling(s) from December–February, therefore these locations were removed from analysis. Wd is the width of the flaw lead at the point closest to the bear, ar_dl is the total area and wd_dl is the maximum width of the flaw lead.

Rank	Model	k	AIC_c	ΔAIC_c	w	LL
December–May ($n_{locations}$ = 16 058)						
1	Month + RS + Month*RS + ar_dl + ar_dl^2	19	180312.8	0.0	0.7	-90137
2	Month + RS + Month*RS + wd_dl	18	180314.5	1.8	0.2	-90139
3	Month + RS + Month*RS + wd_dl + wd_dl^2	19	180315.0	2.2	0.2	-90138
4	Month + RS + Month*RS + ar_dl	18	180326.9	14.1	0.0	-90145
5	Month + RS + Month*RS	17	180391.3	78.5	0.0	-90179
December–May Without Locations on Landfast Ice ($n_{locations}$ = 15 864)						
1	Month + RS + Month*RS + ar_dl + ar_dl^2	19	177800	0.0	1.0	-88881
2	Month + RS + Month*RS + wd_dl + wd_dl^2	19	177810	10	0.0	-88886
3	Month + RS + Month*RS + wd_dl	18	177813	13	0.0	-88889
4	Month + RS + Month*RS + ar_dl	18	177816	16	0.0	-88890
5	Month + RS + Month*RS	17	177893	92	0.0	-88929

Table S11. Covariate coefficient estimates for the top models predicting adult female polar bear distance to the western Hudson Bay landfast ice with and without locations on western Hudson Bay landfast ice using a maximum likelihood linear mixed effects model (α = 0.05). YRLG represents females with yearling(s), and solitary represents solitary females. There was only one female with yearling(s) from December–February, therefore these locations were removed from analysis. YRLG was excluded from the December–February model due to small sample size (n_{bears} = 1). Max width is the maximum width of the flaw lead.

				95% CI		
Model	Parameter	Estimate	SE	Lower	Upper	*p* value
December–May With All Locations	December	150.0	4.6	140.9	159.1	<0.001
	January	65.0	3.6	57.9	72.2	<0.001
	February	20.6	3.8	13.3	28.0	<0.001
	March	-19.6	3.7	-26.8	-12.3	<0.001
	April	19.3	3.3	12.7	25.8	<0.001
	COY & May	159.7	10.7	138.7	180.7	<0.001
	Solitary	-8.6	3.3	-15.1	-2.1	<0.01
	YRLG	-9.1	3.6	-16.1	-2.0	<0.05
	Width	-2.2E-04	2.5E-05	-2.7E-04	-1.7E-04	<0.001
	Dec*Solitary	-77.9	15.0	-107.3	-48.4	<0.001
	Jan* Solitary	-0.03	6.3	-12.4	12.3	>0.05
	Feb* Solitary	54.8	6.0	43.0	66.5	<0.001
	Mar* Solitary	65.3	4.2	57.0	73.6	<0.001
	Apr* Solitary	20.3	3.9	12.6	28.0	<0.001
	Mar*YRLG	37.0	4.5	28.1	45.8	<0.001
	Apr*YRLG	8.8	4.2	0.5	17.0	<0.05
December–May Without Locations on Landfast Ice	December	155.2	4.5	146.4	164.1	<0.001
	January	71.2	3.5	64.3	78.1	<0.001
	February	26.7	3.6	19.6	33.8	<0.001
	March	-10.4	3.7	-17.6	-3.3	<0.01
	April	24.5	3.2	18.3	30.8	<0.001
	COY & May	155.4	10.7	134.6	176.3	<0.001
	Solitary	-4.3	3.3	-10.8	2.2	>0.05
	YRLG	-2.0	3.6	-9.1	5.0	>0.05
	Area	-3.28E-04	2.08E-04	-7.35E-04	7.90E-05	>0.05
	Area^2	-2.08E-04	4.91E-05	-3.05E-04	-1.12E-04	<0.001
	Dec*Solitary	-90.3	14.9	-119.5	-61.1	<0.001
	Jan*Solitary	-10.6	6.3	-22.9	1.8	>0.05
	Feb*Solitary	46.0	6.0	34.4	57.7	<0.001
	Mar*Solitary	57.4	4.2	49.0	65.7	<0.001
	Apr*Solitary	15.2	3.9	7.6	22.9	<0.001
	Mar*YRLG	28.7	4.5	19.9	37.6	<0.001
	Apr*YRLG	4.5	4.2	-3.8	12.8	>0.05

Supplement 7 Testing Autocorrelation of Data

This supplement contains results of models run on a subset of data to test the effect of autocorrelation. To account for autocorrelation, we retained only 1 location per day for each bear and repeated the distance to the western Hudson Bay flaw lead, habitat quality and floe size models. This resulted in removing 13562, 11033, and 10480 locations for each analysis, respectively. Akaike Information Criterion results are presented in Table S12, and model results are presented in Table S13 and Fig. S4. Subsampling to 1 location per day did not change the results from the models run with all data.

Table S12. Akaike Information Criterion results for the top 5 candidate models predicting adult female polar bear use of habitat quality, floe size, and distance to the western Hudson Bay flaw lead using a generalized linear mixed effect model (GLME) and maximum likelihood linear mixed effects model (LME; $\alpha = 0.05$). Data was subsampled to 1 location per day to account for autocorrelation. Individual bear identification was the random effect. k is the number of random effects terms, AIC_c is the corrected Akaike Information Criterion score for each model, ΔAIC_c is the difference in AIC_c scores between the top model and subsequent candidate models, w is the AIC_c weight, and LL is the log likelihood value. dist_ld represents the bears' distance to the western Hudson Bay flaw lead. Month represents 6 categories (December–May inclusive). RS represents reproductive status with 3 categories; females with cub(s)-of-the-year (Dec: $n_{bears} = 21$; Jan: $n_{bears} = 23$; Feb: $n_{bears} = 20$; Mar: $n_{bears} = 20$; Apr: $n_{bears} = 17$; May: $n_{bears} = 16$), females with yearling(s; Mar: $n_{bears} = 24$; Apr: $n_{bears} = 26$; May: $n_{bears} = 23$), and solitary females (Dec: $n_{bears} = 2$; Jan: $n_{bears} = 4$; Feb: $n_{bears} = 5$; Mar: $n_{bears} = 39$; Apr: $n_{bears} = 39$; May: $n_{bears} = 31$). There was only one female with yearling(s) from December–February, therefore these locations were removed from analysis. Wd is the width of the flaw lead at the point closest to the bear, ar_dl is the total area and wd_dl is the maximum width of the flaw lead.

Rank	Model	k	AIC_c	ΔAIC_c	w	LL
Habitat Quality (GLME; $n_{locations} = 2496$)						
1	dist_ld	3	152	0.0	0.7	-73
2	dist_ld + $dist\_ld^2$	4	154	2.0	0.3	-73
Floe Size (GLME; $n_{locations} = 2483$)						
1	dist_ld	3	401	0.0	0.7	-197
2	dist_ld + $dist\_ld^2$	4	402	1.0	0.3	-197
December–May (LME; $n_{locations} = 2956$)						
1	Month + RS + Month*RS + wd_dl + wd_dl^2	19	33650	0.0	0.8	-16806
2	Month + RS + Month*RS + wd_dl	18	33653	3.0	0.2	-16808
3	Month + RS + Month*RS + ar_dl + ar_dl^2	19	33656	6.0	0.0	-16809
4	Month + RS + Month*RS + ar_dl	18	33657	7.0	0.0	-16810
5	Month + RS + Month*RS	17	33674	24.0	0.0	-16820

Table S13. Covariate coefficient estimates for the top models predicting adult female polar bear use of habitat quality, floe size, and distance to the western Hudson Bay flaw lead (FL) using a generalized linear mixed effect model (GLME) and maximum likelihood linear mixed effects model (LME; α = 0.05). Data was subsampled to 1 location per day to account for autocorrelation. YRLG represents females with yearling(s), and solitary represents solitary females. There was only one female with yearling(s) from December–February, therefore these locations were removed from analysis. YRLG was excluded from the December–February model due to small sample size ($n_{bears} = 1$). Distance to FL is the bears' distance to the FL. Width is the maximum daily width of the flaw lead.

				95% CI		
Model	Parameter	Estimate	SE	Lower	Upper	*p* value
Habitat Quality (GLME)	Distance to FL	0.04	0.01	0.03	0.05	<0.001
	Constant	5.34	1.45	2.51	8.18	<0.001
Floe Size (GLME)	Distance to FL	0.01	0.001	0.008	0.01	<0.001
	Constant	10.46	1.54	7.43	13.49	<0.001
Distance to FL (LME)	December	133.6	4.7	124.3	142.8	<0.001
	January	62.9	3.7	55.6	70.2	<0.001
	February	20.4	3.8	12.9	27.9	<0.05
	March	-22.8	3.8	-30.2	-15.3	<0.05
	April	14.8	3.4	8.2	21.4	>0.05
	COY & May	163.5	11.2	141.6	185.5	<0.001
	Solitary	1.7	3.4	-4.9	8.2	>0.05
	YRLG	-7.7	3.7	-14.9	-0.5	>0.05
	Width	4.9E-01	4.3E-05	4.9E-01	4.9E-01	<0.001
	$Width^2$	4.3E-04	7.8E-05	2.8E-04	5.8E-04	<0.05
	Dec*Solitary	-85.8	15.2	-115.7	-55.9	<0.05
	Jan* Solitary	-21.6	6.4	-34.2	-9.1	>0.05
	Feb* Solitary	37.5	6.1	25.6	49.4	<0.05
	Mar* Solitary	53.6	4.3	45.2	62.0	<0.001
	Apr* Solitary	13.8	4.0	6.0	21.7	>0.05
	Mar*YRLG	36.3	4.6	27.3	45.2	<0.01
	Apr*YRLG	10.2	4.3	1.8	18.7	>0.05

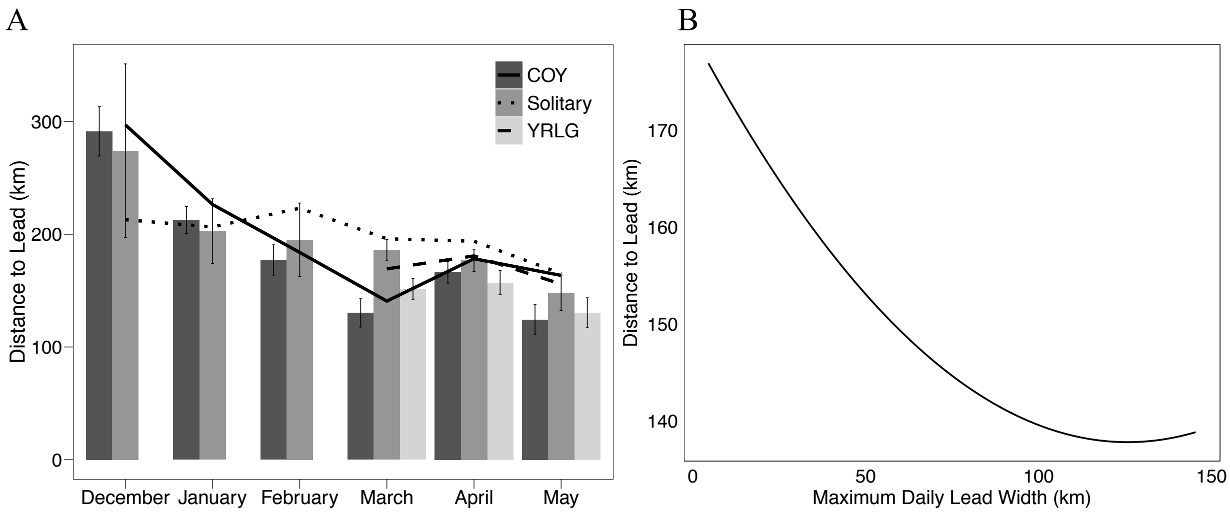

Fig. S4. Response plots predicting polar bear use of the western Hudson Bay FL. A) Predicted distance to the FL (horizontal lines) based on the interaction between month and reproductive status, with bars representing observed values with 95% confidence intervals (vertical lines). B) Predicted distance to the FL based on the maximum daily FL width. YRLG = females with yearling(s), Solitary = solitary females, and COY = females with cub(s)-of-the-year.

Supplement 8 Crossing of the western Hudson Bay flaw lead

This supplement contains a table of all tracks ≤1 median step length from the western Hudson Bay flaw lead with summary statistics related to the trips (Table S14). This supplement also includes candidate models (Table S15) predicting crossing of the flaw lead and results of Akaike Information Criterion (Table S16) used to choose the top model. Results of the top model are presented in Table S17.

Table S14. Adult female polar bear trips on the flaw lead from January 2010–May 2018. Adult female polar bears are from the Western Hudson Bay subpopulation. A trip represents bears locations ≤1 median step length from the, and ends either when the bear moves >1 median step length from the flaw lead, or the end of available flaw lead imagery. Bear ID is the individual bear identification, and RS is the bear reproductive status. Solitary represents a solitary female, COY represents a female with cub(s)-of-the-year, YRLG represents a female with yearling(s), and UNK the reproductive status is unknown. Arrive and leave are the date and time of the first location and last location of the bear on the flaw lead for each trip respectively. Cross start is the date and time of the last location before the bear started crossing the flaw lead, and Cross end is the date and time of the first location on the opposite side of the flaw lead. Mean width is the mean over the whole trip on the flaw lead, cross start width is the width of the flaw lead when the bear began crossing, and width leave is the width of the flaw lead of the last location of the trip. NA indicates bear did not cross the flaw lead. The flaw lead was mapped using synthetic aperture radar.

Bear ID	RS	Arrive	Leave	Cross Start	Cross End	Mean Width (km)	Cross Start Width (km)	Width Leave (km)	Side
X03486	Solitary	2010-04-25 9:00	2010-04-25 13:00	2010-04-25 13:00	2010-04-25 17:00	0.4	0.6	0.3	Coast
X12208	UNK	2010-01-29 1:00[a]	2010-02-01 5:00	2010-01-31 13:00	2010-02-01 9:00	11.9	11.7	17.9	Coast
X12627	Solitary	2015-04-25 5:00[a]	2015-04-25 5:00	NA	NA	1.0	1.0	1.0	Coast
X17097	UNK	2010-03-11 1:00[a]	2010-03-11 21:00	NA	NA	7.8	7.0	7.1	Bay
X17097	UNK	2010-03-13 9:00	2010-03-13 9:00	NA	NA	7.6	7.6	7.6	Bay
X17097	UNK	2010-03-13 17:00	2010-03-14 17:00	NA	NA	8.4	7.3	11.6	Bay
X17339	Solitary	2016-04-03 1:00	2016-04-03 13:00	2016-04-03 1:00	2016-04-03 13:00	2.1	2.8	2.1	Bay
X17598	UNK	2018-04-14 1:00	2018-04-14 13:00	NA	NA	2.2	2.0	3.1	Bay

Bear ID	RS	Arrive	Leave	Cross Start	Cross End	Mean Width (km)	Cross Start Width (km)	Width Leave (km)	Side
X17598	UNK	2018-04-20 1:00	2018-04-21 9:00	NA	NA	15.4	15.9	15.7	Bay
X17598	UNK	2018-04-21 17:00	2018-04-21 21:00	NA	NA	15.0	15.0	15.1	Bay
X17598	UNK	2018-04-22 9:00	2018-04-22 9:00	NA	NA	15.5	15.5	15.5	Bay
X17598	UNK	2018-04-23 21:00	2018-04-24 21:00	NA	NA	19.5	20.1	20.0	Bay
X17598	UNK	2018-05-14 17:00	2018-05-14 17:00	NA	NA	3.4	3.4	3.4	Bay
X17598	UNK	2018-05-15 5:00	2018-05-15 5:00	NA	NA	4.2	4.2	4.2	Bay
X17598	UNK	2018-05-15 13:00	2018-05-15 21:00	NA	NA	4.4	4.4	4.4	Bay
X19143	COY	2017-03-06 17:00[b]	2017-03-06 21:00	2017-03-06 21:00	2017-03-07 1:00	0.5	0.5	0.5	Coast
X19143	YRLG	2018-04-06 3:00	NA	2018-04-07 3:00	2018-04-07 11:00	1.7	1.7	NA	Coast
X19295	COY	2014-03-07 1:00	2014-03-10 13:00	2014-03-10 5:00	2014-03-10 13:00	2.5	1.4	5.5	Coast
X19389	COY	2016-03-31 1:00	2016-04-02 17:00	2016-04-01 17:00	2016-04-02 1:00	8.9	4.1	13.4	Coast
X19602	Solitary	2011-04-13 5:00	2011-04-13 21:00	NA	NA	10.7	11.4	10.5	Bay
X19602	Solitary	2011-04-17 1:00[c]	2011-04-18 13:00	2011-04-18 1:00	2011-04-18 13:00	12.7	17.4	10.2	Bay
X19602	Solitary	2011-04-18 13:00[c]	2011-04-19 5:00	NA	NA	8.5	10.2	7.1	Coast
X19602	Solitary	2011-04-19 13:00	2011-04-20 5:00	2011-04-19 21:00	2011-04-20 9:00	3.7	2.4	5.3	Coast
X19602	Solitary	2011-04-20 13:00	2011-04-20 13:00	NA	NA	11.4	11.4	11.4	Bay
X19602	Solitary	2011-04-26 5:00	2011-04-26 21:00	NA	NA	11.7	12.4	12.0	Bay
X19602	Solitary	2011-05-08 1:00	NA	2011-05-08 21:00	2011-05-10 21:00	30.3	3.1	NA	Bay
X19602	Solitary	2011-05-14 21:00	2011-05-14 21:00	NA	NA	0.9	0.9	0.9	Coast
X19602	Solitary	2011-05-15 21:00	2011-05-16 1:00	NA	NA	0.8	0.8	0.8	Coast
X19602	Solitary	2011-05-16 13:00	2011-05-16 17:00	2011-05-16 9:00	2011-05-16 17:00	0.7	0.8	0.7	Coast
X19602	COY	2012-03-24 5:00	2012-03-24 9:00	2012-03-24 5:00	2012-03-24 9:00	1.1	1.1	1.1	Coast
X19602	COY	2012-05-04 5:00	2012-05-04 5:00	2012-05-04 1:00	2012-05-04 5:00	1.0	1.0	1.0	Bay
X19602	COY	2012-05-04 5:00	2012-05-04 5:00	2012-05-04 5:00	2012-05-04 9:00	1.0	1.0	1.0	Coast
X19627	Solitary	2015-05-02 13:00	2015-05-02 17:00	NA	NA	15.0	15.3	14.7	Bay

Bear ID	RS	Arrive	Leave	Cross Start	Cross End	Mean Width (km)	Cross Start Width (km)	Width Leave (km)	Side
X19627	Solitary	2015-05-03 1:00	2015-05-03 1:00	NA	NA	15.2	15.2	15.2	Bay
X19627	Solitary	2015-05-03 9:00	2015-05-04 5:00	2015-05-03 9:00	2015-05-04 9:00	13.0	14.5	17.0	Bay
X19654	COY	2013-03-26 1:00	2013-03-26 17:00	2013-03-26 9:00	2013-03-26 17:00	2.6	3.2	2.7	Coast
X19826	YRLG	2015-04-23 9:00	2015-04-23 21:00	NA	NA	3.9	3.8	4.4	Bay
X19826	YRLG	2015-04-25 13:00	2015-04-27 21:00	NA	NA	4.8	5.5	6.7	Bay
X19939	YRLG	2016-05-15 9:00	2016-05-16 5:00	NA	NA	113.3	111.4	108.4	Bay
X19939	Solitary	2017-05-12 1:00	2017-05-12 17:00	NA	NA	4.6	6.9	0.9	Bay
X19939	Solitary	2017-05-13 1:00	2017-05-13 1:00	NA	NA	10.7	10.7	10.7	Bay
X19939	Solitary	2017-05-21 1:00	2017-05-21 13:00	NA	NA	21.2	23.5	19.0	Bay
X19939	Solitary	2017-05-21 21:00	2017-05-21 21:00	NA	NA	11.0	11.0	11.0	Bay
X32491	Solitary	2011-02-11 17:00	2011-02-11 17:00	NA	NA	0.8	0.8	0.8	Bay
X33228	YRLG	2018-05-11 17:00	2018-05-11 17:00	2018-05-11 13:00	2018-05-11 17:00	1.5	1.5	1.5	Bay
X33228	YRLG	2018-05-15 17:00	2018-05-15 17:00	NA	NA	1.7	1.7	1.7	Bay
X33326	Solitary	2010-04-18 17:00	2010-04-19 21:00	NA	NA	48.2	51.0	50.1	Bay
X33410	Solitary	2016-05-03 17:00	2016-05-03 21:00	2016-05-03 17:00	2016-05-03 21:00	1.2	0.8	1.5	Bay
X33410	Solitary	2016-05-03 21:00	2016-05-04 1:00	2016-05-04 1:00	2016-05-04 5:00	1.6	1.5	1.8	Coast
X33412	Solitary	2017-05-14 1:00	2017-05-14 1:00	2017-05-14 1:00	2017-05-14 5:00	1.0	1.0	1.0	Bay
X33412	Solitary	2017-05-14 9:00	2017-05-14 9:00	NA	NA	2.5	2.5	2.5	Coast
X33412	Solitary	2017-05-14 17:00	2017-05-14 21:00	NA	NA	3.0	3.0	3.0	Coast
X33412	Solitary	2017-05-16 17:00	2017-05-16 17:00	2017-05-16 17:00	2017-05-16 21:00	0.9	0.9	0.9	Coast
X33412	Solitary	2018-01-20 1:00	2018-01-20 21:00	2018-01-20 13:00	2018-01-20 17:00	2.8	2.8	3.0	Coast
X33510	UNK	2014-03-07 9:00[b]	2014-03-07 17:00	2014-03-07 13:00	2014-03-07 17:00	6.8	4.2	9.9	Coast
X33510	UNK	2014-03-08 1:00[b]	2014-03-08 1:00	NA	NA	23.8	23.8	23.8	Bay
X33510	COY	2015-03-10 5:00[b]	2015-03-10 9:00	2015-03-10 5:00	2015-03-10 9:00	0.9	0.9	0.9	Coast
X33563	YRLG	2014-04-13 9:00	2014-04-13 21:00	NA	NA	9.1	6.2	11.7	Bay

Bear ID	RS	Arrive	Leave	Cross Start	Cross End	Mean Width (km)	Cross Start Width (km)	Width Leave (km)	Side
X33563	YRLG	2014-05-02 5:00	2014-05-02 5:00	NA	NA	1.9	1.9	1.9	Bay
X33563	Solitary	2015-04-16 1:00	2015-04-16 1:00	NA	NA	1.3	1.3	1.3	Coast
X33563	Solitary	2015-04-16 13:00	2015-04-16 21:00	NA	NA	0.9	1.3	0.7	Coast
X33563	Solitary	2015-05-02 1:00	2015-05-02 13:00	NA	NA	1.9	2.7	2.2	Bay
X33563	Solitary	2016-02-15 13:00	2016-02-15 21:00	2016-02-15 13:00	2016-02-15 21:00	2.6	3.3	2.7	Coast
X33579	UNK	2018-04-27 9:00	2018-04-28 5:00	NA	NA	2.5	3.4	1.6	Bay
X33579	UNK	2018-04-28 17:00	2018-04-28 21:00	NA	NA	5.6	4.7	6.4	Bay
X33693	Solitary	2018-05-08 13:00	2018-05-08 21:00	NA	NA	3.3	3.8	2.3	Bay
X33693	Solitary	2018-05-11 1:00	2018-05-11 5:00	NA	NA	0.6	0.6	0.6	Bay
X33693	Solitary	2018-05-11 21:00	2018-05-11 21:00	NA	NA	0.6	0.6	0.6	Bay
X33693	Solitary	2018-05-12 13:00	2018-05-15 1:00	NA	NA	2.7	1.8	3.2	Bay

[a]Bear was already on the flaw lead when flaw lead imagery was available.
[b]Bear was returning to ice from land.
[c]Bear crossed the flaw lead twice before end of trip.

Table S15. Candidate models predicting adult female polar bear crossing of the flaw lead using a generalized linear mixed effects model. A trip represents bears' locations ≤1 median step length from the flaw lead, and ends either when the bear moves >1 median step length from the flaw lead, or the end of available flaw lead imagery. Adult female polar bears are from the Western Hudson Bay subpopulation, from January 2010–May 2018. Month included 3 categories (January–March merged, April, May). January (n_{trips} = 2), February (n_{trips} = 2), and March (n_{trips} = 11) were pooled because of small sample size, and flaw lead width did not significantly differ in these months. Individual bear identification was the random effect. End Width is the flaw lead width when the bear begins crossing, or when the bear leaves the flaw lead without crossing; start width is the flaw lead width for the bear's first location on the flaw lead; and mean width is the mean flaw lead width for the bear's trip on the flaw lead. FL side is the side of the flaw lead (closer to the coast or closer to the middle of the Bay) the bear was on at the beginning of the trip on the flaw lead. The flaw lead was mapped using synthetic aperture radar.

Model	Predictor Variables
Crossing Rate (n_{trips} = 69)	
1	Month
2	End Width
3	End Width + End Width ^{2}
4	Month + End Width
5	Month + End Width + End Width ^{2}
6	Start Width
7	Start Width + Start Width^2
8	Month + Start Width
9	Month + Start Width + Start Width ^{2}
10	Mean Width
11	Mean Width + Mean Width^2
12	Month + Mean Width
13	Month + Mean Width + Mean Width ^{2}
14	FL Side
15	FL Side + Month
16	FL Side + End Width
17	FL Side + End Width + End Width ^{2}
18	FL Side + Mean Width
19	FL Side + Mean Width + Mean Width ^{2}
20	FL Side + Start Width
21	FL Side + Start Width + Start Width ^{2}
22	FL Side + Month + End Width
23	FL Side + Month + End Width + End Width ^{2}
24	FL Side + Month + Mean Width
25	FL Side + Month + Mean Width + Mean Width ^{2}
26	FL Side + Month + Start Width
27	FL Side + Month + Start Width + Start Width ^{2}

Table S16. Akaike Information Criterion results for top 5 candidate models predicting adult female polar bear crossing of the flaw lead using a generalized linear mixed effects model. A trip represents bears' locations ≤1 median step length from the flaw lead, and ends either when the bear moves >1 median step length from the flaw lead, or the end of available flaw lead imagery. Adult female polar bears are from the Western Hudson Bay subpopulation, from January 2010–May 2018. January (n_{trips} = 2), February (n_{trips} = 2), and March (n_{trips} = 11) were pooled because of small sample size, and flaw lead width did not significantly differ in these months. Individual bear identification was the random effect. k is the number of fixed effect terms, AIC_c is the corrected Akaike Information Criterion score for each model, ΔAIC_c is the difference in AIC_c scores between the top model and subsequent candidate models, w is the AIC_c weight, and LL is the log likelihood value. Month has 3 categories, January–March, April, and May. End width is the flaw lead width when the bear begins crossing, or when the bear leaves the flaw lead without crossing; and start width is the width of the flaw lead closest to the bear's first location of the trip on the flaw lead. FL side is the side of the flaw lead (closer to the coast or closer to the middle of the Bay) the bear was on at the beginning of the trip on the flaw lead. The flaw lead was mapped using synthetic aperture radar.

Rank	Model	k	AIC_c	ΔAIC_c	w	LL
All Trips on Flaw Lead (n_{trips} = 68)						
1	Month + End Width	5	75.6	0.0	0.2	-32.3
2	Month + End Width + FL Side	6	77.2	1.7	0.1	-31.9
3	Month + Start Width	5	77.4	1.9	0.1	-33.2
4	Month + End Width + End Width^2	6	77.8	2.3	0.1	-32.2
5	FL + End Width	4	78.1	2.5	0.1	-34.7

Table S17. Covariate coefficient estimates for the top generalized linear mixed effects models predicting adult female polar bear crossing of the western Hudson Bay flaw lead (FL) when polar bears were ≤3.3 km from the FL (α = 0.05). Width end = width of the FL closest to the bear when the bear either begins crossing the FL or moves > 3.3 km from the FL without crossing.

				95% CI		
Dependent Variable	Parameter	Estimate	SE	Lower	Upper	*p* value
FL Crossing	March	1.34	1.43	-1.47	4.15	>0.05
	April	-3.89	2.11	-8.02	0.24	>0.05
	May	-3.87	2.39	-8.56	0.83	>0.05
	Width End	-2.4E-04	1.2E-04	-4.8E-04	-2.4E-06	<0.05

Supplement 9 First passage time

This supplement contains methods and results for comparing 4 spatial intervals to interpolate points along the tracks of Western Hudson Bay polar bears to find the spatial scale (radius) of area-restricted search (Table S18). This radius was used to calculate first passage time (FPT) on the tracks. This supplement also contains a figure (Fig. S5) depicting the mean variance in $\log_{10}$-transformed first passage time, and tables containing the candidate models (Table S19), and the Akaike information criterion results (Table S20) of models predicting first passage time of Western Hudson Bay adult female polar bears, as well as results of models run with and without locations on western Hudson Bay landfast ice (Table S21).

To determine the best spatial interval for calculating the radius of area-restricted search, points were interpolated at equal spatial intervals along five tracks from two adult female polar bears from the Western Hudson Bay subpopulation. Spatial intervals for interpolated points were generated at 1 km, 2 km, the median step length, and 5 km, and tested whether the resulting FPT significantly differed using a Spearman's rank correlation coefficient.

Using a spatial scale of 1 km, 2km, 3.3 km (median step length; see section "Results: Bear Movements"), and 5 km did not significantly change the resulting FPT (Table S18).

Table S18. Comparison of 4 different spatial scales for estimating even interval tracks to calculate the radius of peak variance in $\log_{10}$-transformed first passage time of adult female polar bears using a Spearman's rank correlation coefficient. Five tracks from two adult female polar bears from the Western Hudson Bay subpopulation were used ($\alpha = 0.05$).

	2 km		1 km		5 km	
	r	*p* value	r	*p* value	r	*p* value
3.3 km	0.95	<0.001	0.92	<0.001	0.93	<0.001
2 km			0.98	<0.001	0.87	<0.001
1 km					0.84	<0.001

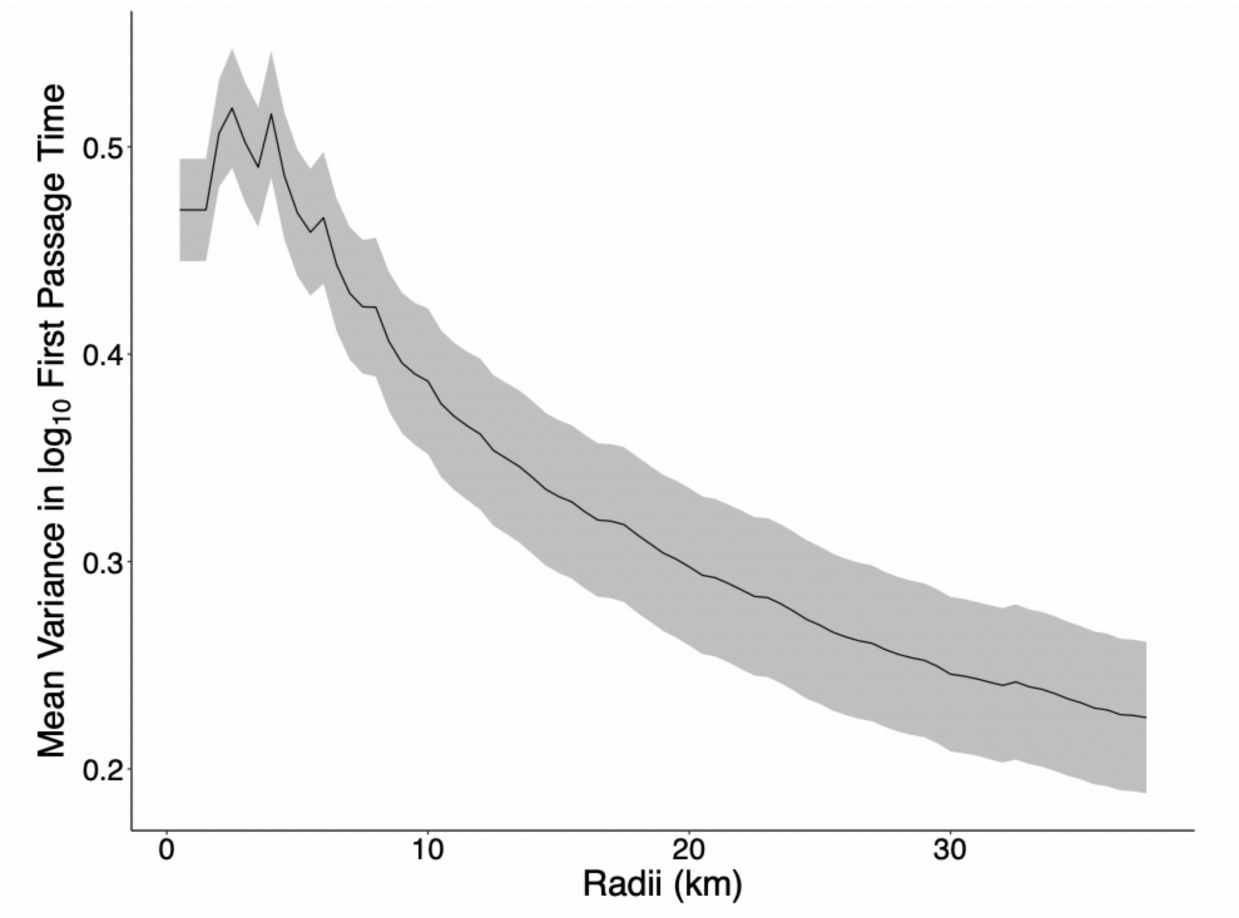

Fig. S5. Mean variance in $\log_{10}$-transformed first passage time (solid black line) with 95% confidence interval (grey) for all western Hudson Bay adult female polar bears from December–May, 2009–2018. First passage time is the amount of time for the bear to cross a circle of a given radius. Peak variance in $\log_{10}$-transformed first passage time is the spatial scale at which the bear undergoes area-restricted search. Peak variance occurred for all tracks for all bears at a radius of 2.5 km.

Table S19. Candidate models predicting adult female polar bear log_{10}-transformed first passage time using a linear mixed effects model. Adult female polar bears are from the Western Hudson Bay subpopulation, from December–May, 2009–2018 for the main model, and January–May, 2010–2018for the on the flaw lead model (when bears were ≤1 median step length from the flaw lead). Individual bear identification was the random effect. January and February were pooled when predicting first passage time on the flaw lead due to small sample size ($n_{locations}$ = 5), and all points were within 26 days. Month included 6 categories for the December–May models (December–May), and 4 categories for the on the flaw lead models (Jan/Feb–May inclusive). RS represents reproductive status with 3 categories; females with cub(s)-of-the-year (Dec: n_{bears} = 12; Jan: n_{bears} = 13; Feb: n_{bears} = 15; Mar: n_{bears} = 14; Apr: n_{bears} = 12; May: n_{bears} = 12), females with yearling(s; Mar: n_{bears} = 13; Apr: n_{bears} = 14; May: n_{bears} = 14), and solitary females (Jan: n_{bears} = 3; Feb: n_{bears} = 4; Mar: n_{bears} = 30; Apr: n_{bears} = 28; May: n_{bears} = 20). There were only one solitary female and female with yearling(s) from December and December–February respectively, therefore these locations were removed from the December–May model. wd is the width of the flaw lead at the point closest to the bear, ar_dl is the total area and wd_dl is the maximum width of the flaw lead. The flaw lead was mapped using synthetic aperture radar.

Model	Predictor Variables
December–May	
1	Month
2	dist_ld
3	dist_ld + dist_ld^2
4	Month + dist_ld
5	Month + dist_ld + dist_ld^2
6	RS
7	Month + RS
8	RS+ dist_ld
9	RS+ dist_ld + dist_ld^2
10	Month + RS+ dist_ld
11	Month + RS+ dist_ld + dist_ld^2
12	Month*RS
13	Month*RS + dist_ld
14	Month*RS + dist_ld + dist_ld^2
On the Flaw Lead	
1	dist_ld
2	dist_ld + dist_ld^2
3	wd
4	wd + wd^2
5	dist_ld + wd
6	dist_ld + dist_ld^2 + wd + wd^2
7	dist_ld + wd + wd^2
8	dist_ld + dist_ld^2 + wd

9	Month
10	Month + dist_ld
11	Month + dist_ld + dist_ld^2
12	Month + wd
13	Month + wd + wd^2
14	RS
15	Month + RS
16	RS + dist_ld
17	RS + dist_ld + dist_ld^2
18	RS + wd
19	RS + wd + wd^2
20	Month + dist_ld + wd
21	Month + dist_ld + dist_ld^2 + wd
22	Month + dist_ld + wd + wd^2
23	Month + dist_ld + dist_ld^2 + wd + wd^2
24	RS + dist_ld + wd
25	RS + dist_ld + dist_ld^2 + wd
26	RS + dist_ld + wd + wd^2
27	RS + dist_ld + dist_ld^2 + wd + wd^2
28	Month + RS + dist_ld
29	Month + RS + dist_ld + dist_ld^2
30	Month + RS + wd
31	Month + RS + wd + wd^2
32	Month + RS + dist_ld + wd
33	Month + RS + dist_ld + dist_ld^2 + wd
34	Month + RS + dist_ld + wd + wd^2
35	Month + RS + wd + wd^2 + dist_ld + dist_ld^2
36	Month*RS

Table S20. Akaike Information Criterion results for the top 5 candidate models predicting adult female polar bear $\log_{10}$-transformed first passage time with and without locations on western Hudson Bay landfast ice using a linear mixed effects model. Polar bears are from the Western Hudson Bay subpopulation, from December–May, 2009–2018, and January–May, 2010–2018for the on the flaw lead model (when bears were ≤1 median step length from the flaw lead). Individual bear identification was the random effect. January and February were pooled when predicting first passage time on the flaw lead due to small sample size (n_{FPTs} = 5), and all points were within 26 days. k is the number of fixed effect terms, AIC_c is the corrected Akaike Information Criterion score for each model, ΔAIC_c is the difference in AIC_c scores between the top model and subsequent candidate models, w is the AIC_c weight, and LL is the log likelihood value. Month included 6 categories for the December–May models (December–May), and 4 categories for the on the flaw lead models (Jan/Feb–May inclusive). RS represents reproductive status with 3 categories; females with cub(s)-of-the-year (Dec: n_{bears} = 12; Jan: n_{bears} = 13; Feb: n_{bears} = 15; Mar: n_{bears} = 14; Apr: n_{bears} = 12; May: n_{bears} = 12), females with yearling(s; Mar: n_{bears} = 13; Apr: n_{bears} = 14; May: n_{bears} = 14), and solitary females (Jan: n_{bears} = 3; Feb: n_{bears} = 4; Mar: n_{bears} = 30; Apr: n_{bears} = 28; May: n_{bears} = 20). There were only one solitary female and female with yearling(s) from December and December–February respectively, therefore these locations were removed from the December–May model. Dist_ld is the bears' distance to the nearest point of the flaw lead, wd is the width of the flaw lead at the point the bear is closest to. The flaw lead was mapped using synthetic aperture radar.

Rank	Model	k	AIC_c	ΔAIC_c	w	LL
December–May (n_{FPT} = 8848)						
1	Month*RS + dist_ld	17	16299	0.0	0.6	-8132
2	Month*RS + dist_ld + dist_ld^2	18	16299	0.9	0.4	-8132
3	Month*RS	16	16329	31	0.0	-8148
4	Month + RS + dist_ld	11	16340	42	0.0	-8159
5	Month + RS + dist_ld + dist_ld^2	12	16341	42	0.0	-8158
December–May Without Locations on Landfast Ice (n_{FPT} = 8771)						
1	Month*RS + dist_ld	17	16132	0.0	0.7	-8049
2	Month*RS + dist_ld + dist_ld^2	18	16134	2	0.3	-8049
3	Month*RS	16	16168	35	0.0	-8068
4	Month + RS + dist_ld	11	16173	41	0.0	-8076
5	Month + RS + dist_ld + dist_ld^2	12	16175	42	0.0	-8075
On the Flaw Lead (n_{FPT} =125)						
1	wd	4	199	0.00	0.3	-95
2	Month + wd	7	201	2	0.2	-92

3	wd + dist_ld	5	201	2	0.1	-95
4	wd + wd^2	5	201	2	0.1	-95
5	RS + wd	6	201	2	0.1	-94
On the Flaw Lead Without Locations on Landfast Ice (n_{FPT} =106)						
1	Month + wd	7	166	0.0	0.3	-75
2	Month + wd + dist_ld	8	167	0.8	0.2	-75
3	Month + wd + wd^2	8	168	2.3	0.1	-75
4	Month + wd + dist_ld + $dist\_ld^2$	9	169	2.8	0.1	-75
5	Month + wd + wd^2 + dist_ld + $dist\_ld^2$	9	169	3.1	0.1	-75

Table S21. Covariate coefficient estimates for the top maximum likelihood linear mixed effects models predicting adult female polar bear $\log_{10}$-transformed first passage time with and without locations on western Hudson Bay landfast ice. Polar bears are from the Western Hudson Bay subpopulation from December–May, 2009–2018 for the main model, and January–May, 2010–2018for the on the flaw lead model (when bears were ≤1 median step length from the flaw lead). January and February were pooled when predicting first passage time on the flaw lead due to small sample size ($n_{FPT} = 5$), and all points were within 26 days. Solitary represents solitary adult females, and YRLG represents females with yearling(s). There were only one solitary female and female with yearling(s) from December and December–February respectively, therefore these locations were removed from the December–May model. Distance to FL is the distance of the polar bear to the flaw lead. FL width is the width of the flaw lead at the closest point to the polar bear ($\alpha = 0.05$). The flaw lead was mapped using synthetic aperture radar.

				95% CI		
Model	Parameter	Estimate	SE	Lower	Upper	*p* value
First Passage Time With All Locations	December	-0.13	0.06	-0.23	-0.02	<0.05
	January	-0.02	0.04	-0.10	0.05	>0.05
	February	0.03	0.04	-0.05	0.11	>0.05
	March	0.03	0.04	-0.05	0.10	>0.05
	May	-0.08	0.04	-0.16	-0.01	<0.05
	COY & April	1.78	0.04	1.70	1.85	<0.001
	Solitary	-0.19	0.03	-0.25	-0.1287	<0.001
	YRLG	-0.18	0.04	-0.25	-0.11	<0.001
	Distance to FL	6.0E-07	1.0E-07	4.0E-07	8.1E-07	<0.001
	Jan*Solitary	-0.23	0.07	-0.37	-0.09	<0.01
	Feb*Solitary	0.27	0.07	0.12	0.41	<0.001
	Mar*Solitary	0.14	0.05	0.06	0.23	<0.01
	May*Solitary	0.12	0.05	0.02	0.21	<0.05
	Mar*YRLG	0.02	0.05	-0.08	0.12	>0.05
	May*YRLG	0.07	0.05	-0.03	0.16	>0.05
First Passage Time Without Landfast Ice Locations	December	-0.14	0.06	-0.24	-0.03	<0.05
	January	-0.03	0.04	-0.10	0.05	>0.05
	February	0.02	0.04	-0.06	0.10	>0.05

	March	0.02	0.04	-0.05	0.10	>0.05
	May	-0.08	0.04	-0.15	-0.01	<0.05
	COY & April	1.78	0.04	1.70	1.86	<0.001
	Solitary	-0.19	0.03	-0.25	-0.13	<0.001
	YRLG	-0.20	0.04	-0.27	-0.12	<0.001
	Distance to FL	0.0007	0.0001	0.0004	0.0009	<0.001
	Jan*Solitary	-0.23	0.07	-0.37	-0.09	<0.01
	Feb*Solitary	0.27	0.07	0.13	0.42	<0.001
	Mar* Solitary	0.15	0.05	0.06	0.24	<0.001
	May* Solitary	0.11	0.05	0.02	0.20	<0.05
	Mar*YRLG	0.03	0.05	-0.06	0.13	>0.05
	May*YRLG	0.07	0.05	-0.03	0.17	>0.05
First Passage Time On FL Without Locations on Landfast Ice	February	0.50	0.25	0.01	1.00	<0.05
	March	0.84	0.25	0.35	1.33	<0.01
	April	0.15	0.13	-0.12	0.41	>0.05
	May	1.62	0.12	1.39	1.86	<0.001
	FL Width	-3.8E-06	1.0E-06	-5.8E-06	-1.9E-06	<0.001

Supplement 10 von Mises Distributions of Relative movement directions and Turning Angles

This supplement contains a table presenting the prominent relative movement directions and turning angles of Western Hudson Bay adult female polar bears relative to the distance to the western Hudson Bay flaw lead (Table S22), calculated with and without locations on western Hudson Bay landfast ice, as well as Fig. S6 of the von Mises distributions of angles calculated without locations on western Hudson Bay landfast ice.

Table S22. Log likelihood ratio results of the best fit von Mises model for the adult female polar bear movements relative to the flaw lead and turning angles from December–May, 2009–2018 with and without locations on western Hudson Bay landfast ice. Adult female polar bears are from the Western Hudson Bay subpopulation from December–May, 2009–2018. μ is the mean of the peak and k is the kappa. The bolded μ is the most prominent peak. Relative movement directions were divided into 3 groups: towards (–45° ≤ θ ≤ 45°), along (–45° > θ > –135°) and (45° < θ < 135°), and away (–135° ≤ θ ≥ 135°) from the flaw lead. Turning angles were divided into 3 groups: low (–45° ≤ θ ≤ 45°), turn (–45° > θ > –135° & 45° < θ < 135°), and reversal turn (–135° ≤ θ ≥ 135°; α = 0.05). Bear locations were divided into 3 distance categories: 'on' (≤1 median step length from the flaw lead), 'near' (>1 step length, ≤2 times median daily displacement from the flaw lead), and 'off' (>2 times median daily displacement from the flaw lead). The flaw lead was mapped using synthetic aperture radar.

		μ_1	k_1	μ_2	k_2	Prominent Angle	χ^2	df	*p* value
Movement Relative to the Flaw Lead									
All Locations	On	**101**	4.7	-69	0.2	Along	11	5	<0.05
	Near	160	0.3	**-23**	4.4	Towards	17	5	<0.01
	Off	149	1.4	**-31**	1.9	Towards	2167	5	<0.001
Without Locations on Landfast Ice	On	111	0.5	**-48**	10.2	Along	15	5	<0.05
	Near	156	0.3	**-26**	3.9	Towards	13	5	<0.05
	Off	149	1.4	**-31**	1.9	Towards	2176	5	<0.001
Turning Angles									
All Locations	On	**16**	3.0	-142	0.5	Low	52	5	<0.001
	Near	129	0.5	**22**	2.9	90 Deg	20	5	<0.001
	Off	**9.6**	6.4	36	0.6	Low	2941	5	<0.001
Without Locations on Landfast Ice	On	**18**	2.6	-163	0.7	Low	52	5	<0.001
	Near	**25**	3.6	124	0.5	90 Deg	96	5	<0.001
	Off	**10**	6.5	36	0.6	Low	2920	5	<0.001

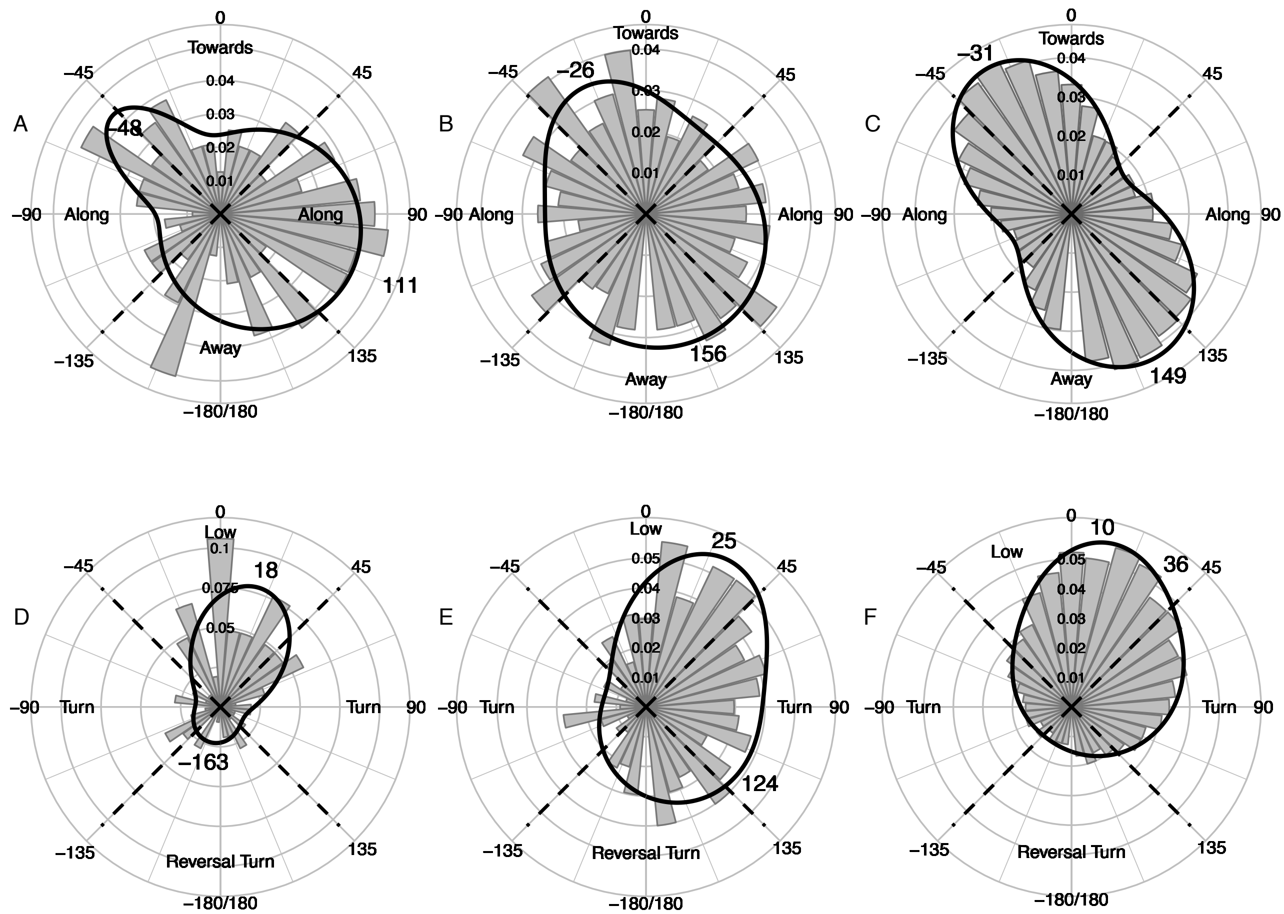

Fig. S6. Direction of movements of adult female polar bears relative to the flaw lead and turning angles from December–May, 2009–2018 without locations on western Hudson Bay landfast ice. Bear locations were divided into 3 distance categories: 'on' (≤1 median step length from the flaw lead), 'near' (>1 step length, ≤2 times median daily displacement from the flaw lead), and 'off' (>2 times median daily displacement from the flaw lead) the flaw lead. Adult female polar bears are from the Western Hudson Bay polar bear subpopulation. Relative movement directions were divided into 3 groups: towards (–45° ≤ θ ≤ 45°), along (–45° > θ > –135° & 45° < θ < 135°), and away (–135° ≤ θ ≥ 135°) from the flaw lead. Distributions of relative movement directions were fit a) on the flaw lead, b) near the flaw lead, c) off the flaw lead. Turning angles were divided into 3 groups: low (–45° ≤ θ ≤ 45°), turn (–45° > θ > –135° & 45° < θ < 135°), and reversal turn (–135° ≤ θ ≥ 135°). Distributions of turning angle were fit d) on the flaw lead, e) near the flaw lead, f) off the flaw lead. Grey bars represent the proportion of angles, and the solid black line represents the bivariate von Mises distribution with the best fit. The flaw lead was mapped using synthetic aperture radar.

Supplement 11 Interpolating missing locations using a continuous-time correlated random walk

This supplement contains methods and results to test whether interpolating missing locations using a continuous-time correlated random walk (CRAWL) using the Kalman-filter significantly affected the calculation of first passage time (FPT; Fig. S7).

To find the largest permissible time gap to be interpolated using CRAWL without significantly affecting statistical analysis, 10-70% of locations were randomly removed from 5 tracks of 2 Western Hudson Bay polar bears with >250 locations per track. The removed locations were then interpolated using the ‘crawl’ R package (Johnson et al. 2008, Johnson & London 2018). FPT was calculated (See section “Methods: First Passage Time) on the original tracks and the interpolated tracks, and compared by calculating a Spearman’s rank correlation coefficient ($\alpha = 0.05$).

When 50% of the locations were removed from the CRAWL test tracks, the time between consecutive points before interpolation was 8.0 ± 0.2 h. The largest time gap interpolated was 56 h, with a mean time gap of 11.8 ± 0.3 h. FPT was not significantly different between the original track and interpolated track (Spearman’s rank $r = 0.82$, $p < 0.001$, y-intercept = 1.7, m = 0.9; Fig. S7).

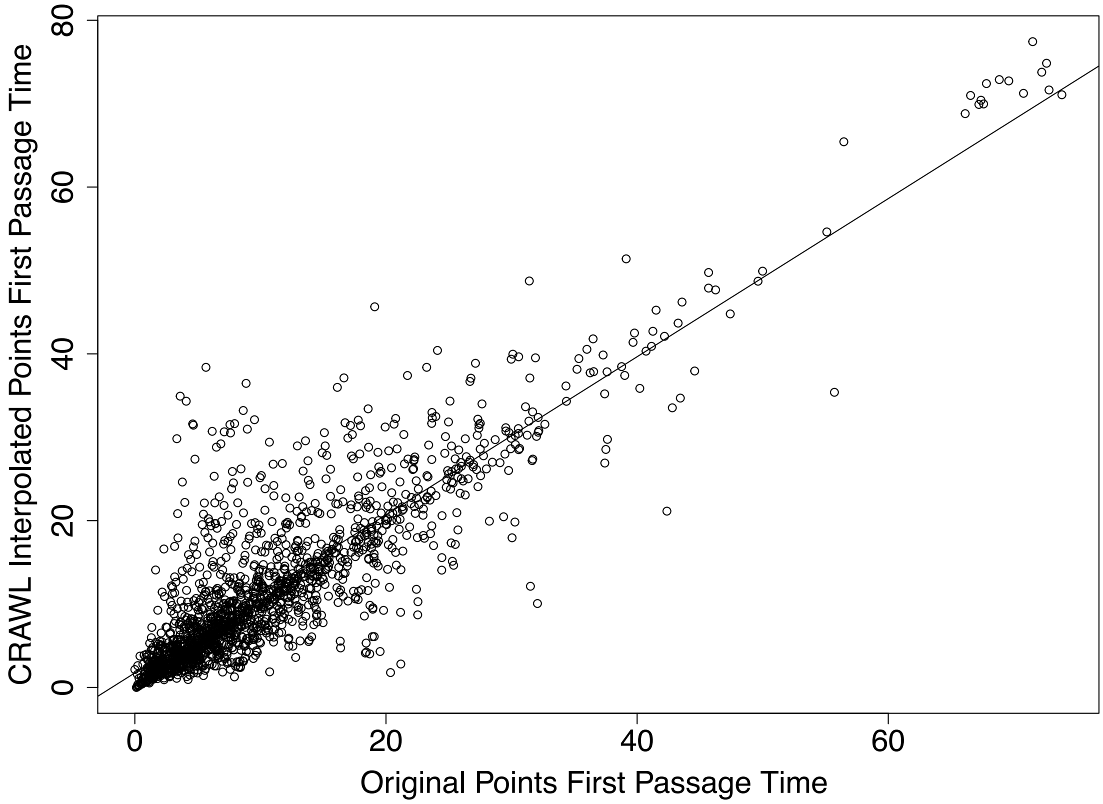

Fig. S7. Comparing first passage time calculated from Western Hudson Bay adult female polar bears' original locations to first passage time calculated from locations where 50% of the bears' track was interpolated using CRAWL. Five tracks from two bears were used. Spearman's rank (r = 0.82, $p < 0.001$; $\alpha = 0.05$).

LITERATURE CITED

Burnham KP, Anderson DR (2002) Model selection and multimodel inference: A practical information-theoretic approach, 2nd edn. Springer, New York

Canadian Ice Service (2009) Canadian Ice Service Arctic regional sea ice charts in SIGRID-3 format, version 1. 2009-2018. Boulder, Colorado USA. NSIDC: National Snow and Ice Data Center: https://doi.org/10.7265/N51V5BW9. July 7, 2019.

Johnson DS, London JM (2018) Crawl: An R package for fitting continuous-time correlated random walk models to animal movement data. Zenodo

Johnson DS, London JM, Lea M-A, Durban JW (2008) Continuous-time correlated random walk model for animal telemetry data. Ecology 89:1208-1215

Ramsay M, Andriashek D (1986) Long distance route orientation of female polar bears (*Ursus maritimus*) in spring. J Zool 208:63-72

Stirling I, Jonkel C, Smith P, Robertson R, Cross D (1977) The ecology of the polar bear (*Ursus maritimus*) along the western coast of Hudson Bay, Vol 33. Minister of Supply and Services